

## Using remote sensing to investigate erosion rate variability in a semiarid watershed, due to changes in vegetation cover

**JAIME GARATUZA-PAYÁN, RAQUEL SÁNCHEZ-ANDRÉS, SALVADOR SÁNCHEZ-CARRILLO & JOSE M. NAVARRO**

*Department of Water and Environmental Sciences, Instituto Tecnológico de Sonora, 5 de Febrero 818 Sur, Ciudad Obregón, Sonora CP-85000, Mexico*

[garatuza@itson.mx](mailto:garatuza@itson.mx)

**Abstract** The vegetation cover status of a watershed is a key control of erosion intensity. Any management plan must therefore take into account temporal changes in surface condition within a watershed. The type and condition of the vegetation cover are the most important watershed characteristics affected by seasonal and inter-annual changes. In order to explore these effects further, a study was undertaken in the 74 532 km<sup>2</sup> Yaqui River basin. Ten Landsat scenes covering the three seasons in 1976, 1983 and 1992 were used to assess inter-annual changes in surface cover over the Yaqui catchment, while monthly composites of NOAA-AVHRR NDVI images were employed to evaluate intra-annual or seasonal changes in the vegetation cover. Maps of vegetation type and density, based on satellite images, were used to derive distributed estimates of the vegetation cover factor in the Universal Soil Loss Equation. The results show that vegetation cover is closely related to seasonal precipitation variability and to the inter-annual variability associated with global scale phenomena such as ENSO. The study demonstrates the usefulness of distributed estimates of erosion potential for improving understanding of the relationships between vegetation cover and erosion in semiarid watersheds and as a tool for improved catchment management.

**Key words** erosion; Mexico; remote sensing; semiarid areas; vegetation cover

### INTRODUCTION

Soil erosion can be defined as the translocation of soil particles by processes which are influenced by climate, soil, topography and vegetation cover. Human activity increases, decreases or stops the operation of these natural processes (Bork & Frielinghaus, 1997). Runoff and sediment production from a watershed are highly variable, both in time and space. This variability reflects differences in surface condition over spatial scales ranging from the basin to the local scale, as well as changes in seasonal rainfall. Auzet *et al.* (1995) reported a close correlation between runoff contributing area and the surface condition of the catchment.

The revised Universal Soil Loss Equation (RUSLE) has widely been used for predicting mean annual soil loss for specific areas. In this equation, soil loss  $A$  is defined as the product of the rainfall/runoff erosivity factor  $R$ , the soil erodibility factor  $K$ , a slope steepness factor  $S$ , a slope length factor  $L$ , a cover management factor  $C$ , and a supporting practices factor  $P$  (Renard *et al.*, 1997), i.e.:

$$A = R K S L C P \quad (1)$$

Modelling soil erosion is a complex task, because soil loss is influenced not only by multiple factors, but also by the interactions between the factors and inputs from other systems. Furthermore, soil loss varies in both space and time, because of the heterogeneity of the factors at different spatial and temporal scales (e.g. Wu & Loucks, 1995; Marceau & Hay, 1999; Wu, 1999). The spatial and temporal variability of the input factors in the soil erosion system may be very large, and the sensitivity of predicted soil loss to this variability can vary considerably in both space and time. Neglecting this variability may lead to large errors in the prediction of soil loss, which may in turn compromise decision making.

There is therefore a need to develop a strategy to provide decision-makers with spatially and temporally variable estimates of soil loss and its controlling factors. The study reported here presents a strategy for achieving this and provides an example of its application to the cover factor, *C*. The objective of the study is to demonstrate the application of remote sensing in investigating the spatial and temporal variability of erosion, by modelling the spatial and temporal variability of the input factors and deriving estimates for any given location and time. It has been applied to a case study in which spatial and temporal variations in the cover factor (*C*) have been estimated using remotely sensed data, to derive information on vegetation type and cover density. This paper therefore addresses spatial and temporal variability in erosion processes and sediment production caused by climate and vegetation cover. The research involved monitoring natural vegetation type and cover density with Landsat and AVHRR and evaluating the impact of these specific surface hydrologic conditions on erosion rates. In this manner, the lack of experimental data on soil erosion, so common in semiarid regions, can to a certain extent be overcome, resulting in better prediction of erosion rates.

## STUDY AREA

The study area of the Yaqui River basin is located in northwest Mexico and southwest USA between 27.2° and 31.3°N and 107.1° and 110.6°W (Fig. 1). The basin drains southwestwards to the Gulf of California and embraces considerable diversity within its 74 472 km<sup>2</sup>. Precipitation is highly variable in both space and time and the mean annual values range from 300 mm, close to the coast, to 1400 mm inland. The mean annual runoff is around 2800 × 10<sup>6</sup> m<sup>3</sup> and much of this is stored in three dams with a total capacity of approximately 7000 × 10<sup>6</sup> m<sup>3</sup>, which are used for energy generation, flood control, irrigation, domestic water supply, export to neighbouring basins and recreation. A number of villages and numerous farms are located in the basin. Elevations vary from 150 to over 3000 m a.s.l. The climate is semiarid, with a warm, rainy monsoonal season extending from May to September, followed by a cool season in winter and spring. The mean annual temperature is about 23.4°C with minimum temperatures around -9°C found in the mountains and maximum values above 50°C, close to the coast. Potential evaporation rates are correlated with monthly mean temperatures and are normally higher than the average monthly precipitation. The main soil types in the study area are leptosols (28%), phaeozems (22%), regosols (19%), cambisols (11%) and luvisols (11%). Medium texture soils cover 77% of the area, while fine texture soils cover 19%. The mean organic matter content is 1.7%, with values ranging from 0.2 to 4.1%.

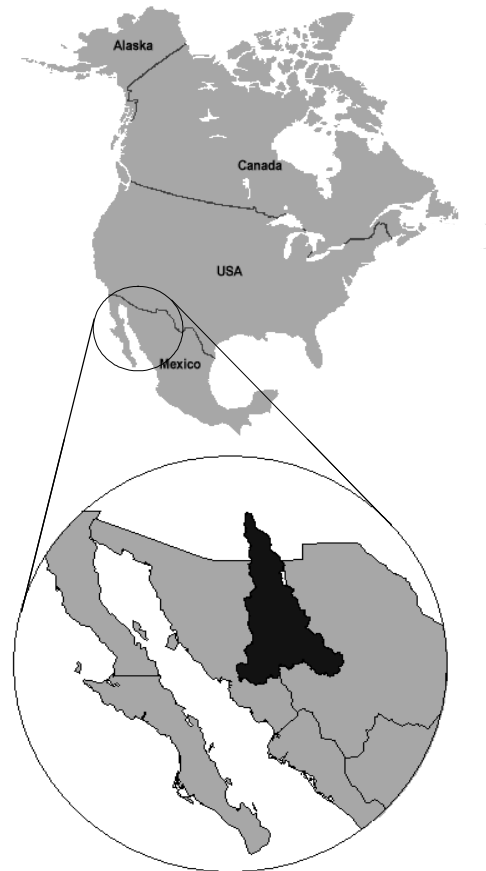


Fig. 1 The location of the Yaqui River watershed.

In general terms, the vegetation of the basin can be described as an ecosystem affected by high grazing pressure, deforestation and occasional fires. Below 2000 m, typical semiarid formations are found (pasture and *Acacia* scrub, *Prosopis*, with *Cactus*). Between 2000 and 2400 m pasture (with a predominance of *Bouteloua hirsute*) and oak forests (*Quercus grisea* and *Q. liminea*) dominate. Pine forests (*Pinus cembroides* and *P. duranguensis*) are the predominant vegetation above 2400 m.

## METHODS

### Spatial and temporal variability of the cover factor, *C*

Analysis of the spatio-temporal variability of the *C* factor was based on Landsat MSS satellite images, NOAA-AVHRR Normalized Vegetation Index (NDVI) images, field sampling and the published tables of Wischmeier & Smith (1978). The land use of the area was classified using multi-spectral and multi-temporal digital image processing of 10 Landsat MSS scenes from three different seasons in 1976, 1983 and 1992. A maximum likelihood method, together with a fuzzy matrix of the spectral wavebands was used to optimize the classification results, in combination with ground truth verification of the test areas. This was based on the criteria defined by Wischmeier & Smith (1978), adapted to the vegetation units present in the study area as a function of vegetation height. Four

classes were defined: crop-grasslands, shrubs lower than 45 cm, shrubs between 45 and 165 cm where deciduous forests were included, and trees higher than 330 cm, where pine and oak forests were included. For each of these vegetation units, an equation was established relating percentage cover to the tabulated values for  $C$  (Wischmeier & Smith, 1978). Finally, NDVI images were used as indicators of the vegetation cover fraction, to derive maps of the  $C$  factor for each vegetation unit. By integrating these maps, a  $C$  factor for the whole basin was obtained.

The temporal variability in potential soil loss was estimated using monthly composites of the vegetation index (NDVI) to sample the seasonal effects of plants and climate. Lower resolution  $0.1^\circ$  NDVI images available from Clark Labs were used to derive the  $C$  factor in a similar way to that used for the high resolution data (Landsat MSS). The RUSLE was used to simulate the soil loss for different  $C$  factor values, reflecting changes in both vegetation type and percentage cover.

### **The variability of other RUSLE variables**

The other RUSLE input variables are the erosivity factor  $R$ , the soil erodibility factor  $K$ , the slope length  $L$ , the steepness factor  $S$  and the conservation practice support factor  $P$ . Values for these factors were derived from different layers of information using IDRISI (Eastman, 2003). The analysis of the spatio-temporal variability of rainfall event characteristics was based on 50 recording and 150 manual measuring stations in the area. In this study, an erosive event was defined as a rainfall with a minimum of 0.5 mm of precipitation. The energy intensity ( $EI$ ) for each single storm event was calculated as the product of the maximum 30 min rainfall intensity ( $\text{mm h}^{-1}$ ) during an event and the sum of the kinetic energy ( $E$ ) for all the 30-min intervals in a storm event, as proposed by Schwertmann *et al.* (1990). The soil erodibility factor  $K$  was estimated, based on erosion relevant properties, such as soil structure, percentage of organic matter and permeability, derived from soil profiles in the watershed and using the modified nomograph method in the RUSLE software (SWCS, 1993). The slope length factor  $L$  combined with the slope steepness factor  $S$  (Wischmeier & Smith, 1978), which is used to quantify the effect of topographic characteristics on soil loss, was derived using a digital elevation model in IDRISI. Values for the conservation practice support factor ( $P$ ) are generally difficult to determine and are the least reliable of all the RUSLE factors (Renard *et al.*, 1991). No specific conservation support practices are applied in the study area; therefore, a default value of 1 was used for the  $P$  factor.

## **RESULTS AND DISCUSSION**

### **Spatial variability of erosion factors**

The spatial variability of the  $R$ ,  $K$  and  $LS$  factors is shown in Fig. 2. The annual rainfall erosivity factor ( $R$ ) ranges from 50 to  $1860 \text{ MJ mm ha}^{-1} \text{ h}^{-1} \text{ year}^{-1}$ , with the lower part and the western edge of the basin showing the higher values, corresponding to the higher rainfall intensities occurring over the western side of the Sierra Madre (Gochis *et al.*, 2003). Most of the area (85%) has low to tolerable erosivity values.

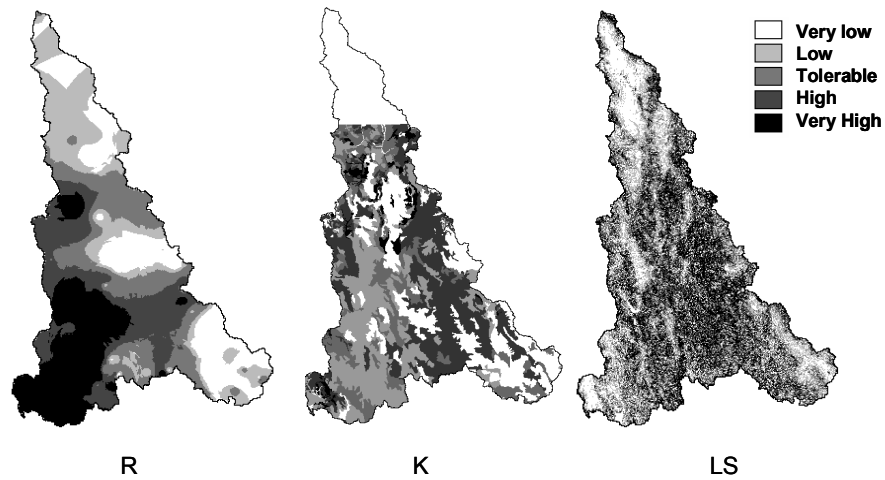


**Fig. 2** Spatial distribution of the  $R$ ,  $K$  and  $LS$  factors. In each case, the whole range was divided into percentiles. The large white strip in the northern part of the  $K$  map is a consequence of the lack of soil data for the US part of the watershed, which was not included in the analysis.

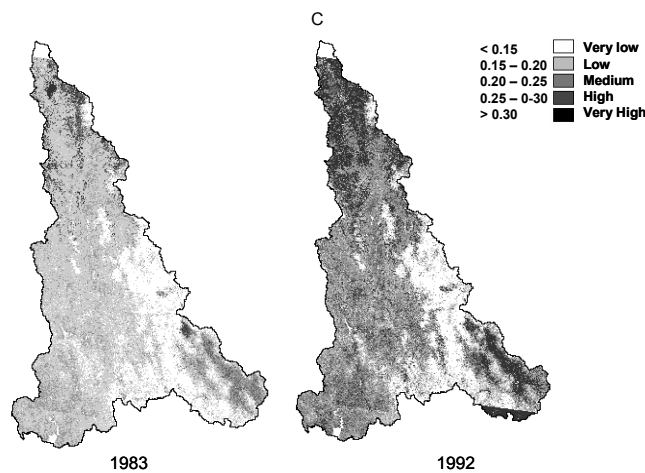


**Fig. 3** Spatial variability of the cover factor ( $C$ ) for two different years (1983 and 1992). The white strip in the north of both maps and the black strip in the southeast corner of the 1992 map represent areas where data are lacking, due to missing data from the remotely sensed vegetation index that is used to derive the  $C$  factor.

The soil erodibility factor ( $K$ ) values reflect the variation of soil types and textures over the watershed. Higher  $K$  values are found along the central ridge, corresponding mainly to luvisols, while lower values are located along the valleys, corresponding to phaeozems.  $K$  values range from 0.04 to 0.07 with 70% of the area characterized by low values. In the case of this factor, soil data were not available for the USA part of the watershed and were therefore not included in the analysis. Topography varies widely across the basin and values for the  $LS$  factor range from 0 to 30, with the lower values covering the flat grasslands to the north and east and the rivers valleys. Based on this factor, 61% of the area is characterized by a low soil loss potential while 27% shows a high risk.

The spatial variability of the cover factor ( $C$ ) for two different years (1983 and 1992) is presented in Fig. 3. Values range from 0 to 0.45 for both years, with the maximum

erosion risk occurring in the north and southeast of the basin, where short vegetation types (grass and shrubs) are present. The generally lower values for 1983 are the consequence of higher NDVI values resulting from a wetter winter as compared to 1992 (the winter rainfall for 1983 was double that for 1992). Land cover in the catchment has changed over the 20-year period from 1973 to 1992, with the forest areas reduced by more than 52 000 ha (1.65% of the forest area in the watershed), with a more drastic reduction occurring during the last decade.

### Spatial and temporal variability of erosion

Figure 4 shows the estimates of soil erosion for the two years. Values range from 0 to over 200 t ha<sup>-1</sup> year<sup>-1</sup> with 42 and 40% of the area having low erosion in 1983 and 1992 respectively (Table 1) and 30 and 34% having high erosion in the same years. There is a slight change in erosion rates towards higher values in 1992 (Table 1 and Fig. 4) as a consequence of the change in cover type and vegetation density resulting in the higher C values showed in Fig. 3.

**Table 1** Percentage distribution of potential soil erosion over the Yaqui River watershed. These values exclude those areas not analysed due to lack of data.

Potential soil erosion (t ha <sup>-1</sup> year <sup>-1</sup> )	Fraction of the watershed	
	1992	1983
Very low <5	19.3	21.6
Low 5–25	20.4	20.6
Medium-low 25–50	11.5	12.2
Medium-strong 50–100	14.8	15.7
Strong 100–200	16.2	18.1
Very strong >200	17.8	11.8

The strong dependence of the estimated soil erosion ( $A$ ) on vegetation density is shown in Fig. 5, where the seasonal variability in  $A$  is shown. Monthly  $A$  maps, based on monthly  $C$  (derived from monthly NDVI) values are presented for 1983. A seasonal pattern can be distinguished with values progressively increasing from January through June, beginning to gradually decrease from July when the rainy season begins and vegetation cover increases, and increasing again in December. The same seasonal behavior is observed during 1992. These maps represent the estimates of annual soil loss derived using the  $C$  values associated with the individual months. Since most (85%) of the rainfall occurs during the summer and this is the period with the most intensive storms, one could expect to have these values in June or July when the soil is most vulnerable due to the small vegetation cover protection (high  $C$  values).

A principal components analysis was undertaken on the erosion rate data sets for both 1983 and 1992. This showed that the first component explained more than 98% of the variance, in both cases with only two classes. These two classes were highly related to the vegetation type indicating that the main source of variability is due to the type and height of the vegetation. These results are similar to those reported by Brath *et al.* (2002)

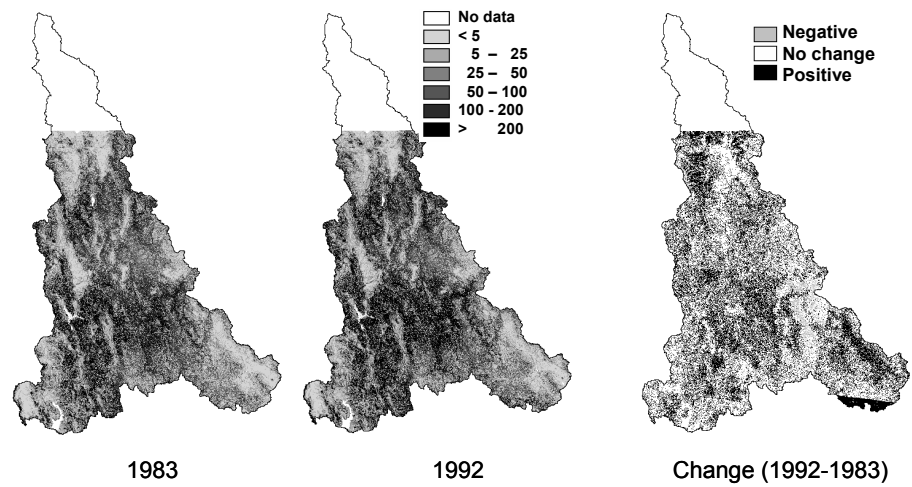


**Fig. 4** Potential soil erosion ( $\text{t ha}^{-1} \text{ year}^{-1}$ ) for 1983 and 1992 and the change over the decade. The large white strip in the north of both maps and the black strip in the southeast corner of the change map represent areas where data are lacking.

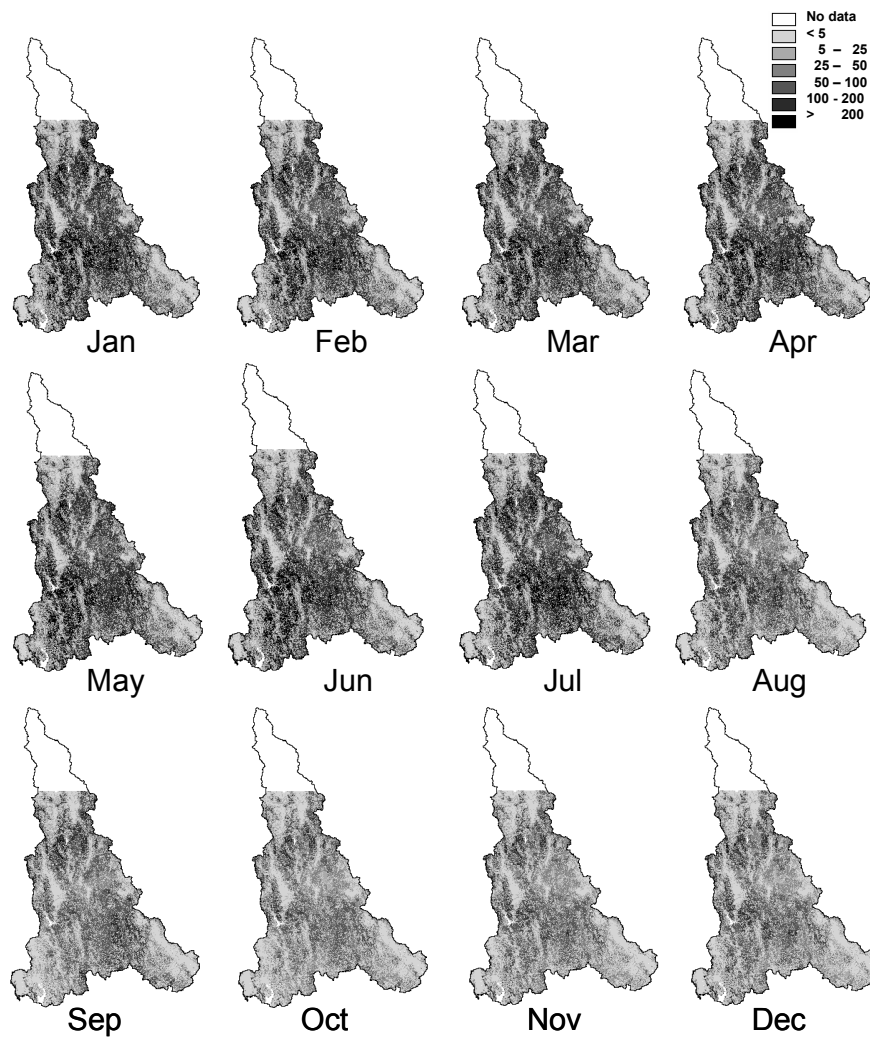


**Fig. 5** Potential soil erosion ( $\text{t ha}^{-1} \text{ year}^{-1}$ ) maps for 1983 derived using the  $C$  values for the individual months.

who used the USLE in a small watershed to show the influence of land-use change on annual gross erosion as well as the increasing vulnerability of upland areas to soil erosion processes during recent decades due to land cover change.

## CONCLUSIONS

The normalized difference vegetation index (NDVI) derived from remote sensing imagery was shown to be an effective tool for estimating seasonal changes in vegetation cover density and the resulting effects on erosion at the basin scale. Erosion rates estimated using MUSLE ranged from 0 to over 200 t ha<sup>-1</sup> year<sup>-1</sup> with around 40–42% and 30–34% of the catchment evidencing strong potential erosion in 1983 and 1992, respectively. Changes in vegetation cover, as measured by NDVI, demonstrated the strong influence of plant phenology on seasonal patterns of erosion. Longer-term changes in vegetation cover and land use caused increased erosion risk, with 6% of the catchment area evidencing erosion rates up to 200 t ha<sup>-1</sup> year<sup>-1</sup>. Vegetation type and height explained more than 98% of the variance of erosion rates.

## REFERENCES

- Auzet, A. V., Boiffin, J. & Ludwig, B. (1995) Concentrated flow erosion in cultivated catchments: influence of soil surface state. *Earth Surf. Processes Landf.* **20**, 759–767.
- Bork, H. R. & Frielinghaus, M. (1997) Zur Tolerierbarkeit von Bodenabtrag. *Mitt. Dtsch. Bodenkdl. Ges.* **83**, 83–86.
- Brath, A., Castellarin, A. & Montanari, A. (2002) Assessing the effects of land-use changes on annual average gross erosion. *Hydrol. Earth System Sci.* **6**(2), 255–265.
- Eastman, J. R. (2003) *Idrisi Kilimanjaro: Tutorial*. Worcester, Clark University, USA.
- Gochis, D. J., Leal, J. C., Shuttleworth, W. J., Watts, C. J. & Garatuza-Payan, J. (2003) Preliminary diagnostics from a new event-based precipitation monitoring system in support of the North American Monsoon Experiment. *J. Hydromet.* **4**, 974–981.
- Marceau, D. J. & Hay, G. J. (1999) Remote sensing contributions to the scale issue. *Can. J. Remote Sens.* **25** (4), 357–366.
- Renard, K. G., Foster, G. R., Weesies, G. A. & Porter, P. J. (1991) RUSLE—revised universal soil loss equation. *J. Soil Water Conserv.* **46**, 30–33.
- Renard, K. G., Foster, C. R., Weesies, G. A., McCool, D. K. & Yoder, D. C. (1997) Predicting soil erosion by water: a guide to conservation planning with the Revised Universal Soil Loss Equation (RUSLE). *USDA Handbook no. 703*. Washington DC, USA.
- Schwertmann, U., Vogl, W. & Kainz, M. (1990) *Bodenerosion durch Wasser—Vorhersage des Abtrags und Bewertung von Gegenmaßnahmen*. Eugen Ulmer Verlag, Stuttgart, Germany.
- Wischmeier, W. H. & Smith, D. D. (1978). Predicting rainfall erosion losses: guide to conservation planning. *US Dept Agric. Handbook no. 282*. Washington DC, USA.
- Woo, M., Fang, G. & di Cenzo, P. (1997) The role of vegetation in the retardation of rill erosion. *Catena* **29**(2), 145–159.
- Wu, J. & Loucks, O. L. (1995) From balance-of-nature to hierarchical patch dynamics: a paradigm shift in ecology. *Quart. Rev. Biol.* **70**, 439–466.
- Wu, J. (1999) Hierarchy and scaling: extrapolating information along a scaling ladder. *Can. J. Remote Sens.* **25**(4), 367–380.